ResearchGate

See discussions, stats, and author profiles for this publication at: https://www.researchgate.net/publication/221809711

Three-Dimensional Organization of Block Copolymers on "DNA-Minimal" Scaffolds

ARTICLE *in* JOURNAL OF THE AMERICAN CHEMICAL SOCIETY · MARCH 2012

Impact Factor: 12.11 · DOI: 10.1021/ja210313p · Source: PubMed

CITATIONS
30

READS
14

8 AUTHORS, INCLUDING:

Manoj Kumar Nayak
Council of Scientific and Industrial Research (…
25 PUBLICATIONS **216** CITATIONS
SEE PROFILE

Karina M M Carneiro
17 PUBLICATIONS **230** CITATIONS
SEE PROFILE

Hassan S. Bazzi
Texas A&M University at Qatar
64 PUBLICATIONS **1,146** CITATIONS
SEE PROFILE

Hanadi F Sleiman
McGill University
110 PUBLICATIONS **3,097** CITATIONS
SEE PROFILE

Available from: Manoj Kumar Nayak
Retrieved on: 17 January 2016

JACS
JOURNAL OF THE AMERICAN CHEMICAL SOCIETY
Article
pubs.acs.org/JACS

Three-Dimensional Organization of Block Copolymers on "DNA-Minimal" Scaffolds

Christopher K. McLaughlin,[†] Graham D. Hamblin,[†] Kevin D. Hänni,[†] Justin W. Conway,[†] Manoj K. Nayak,[‡] Karina M. M. Carneiro,[†] Hassan S. Bazzi,[‡] and Hanadi F. Sleiman*[,†]

[†]Department of Chemistry and Center for Self-Assembled Chemical Structures (CSACS), McGill University, 801 Sherbrooke Street West, Montreal, QC H3A-2K6, Canada

[‡]Department of Chemistry, Texas A&M University at Qatar, P.O. Box 23874, Doha, Qatar

Supporting Information

ABSTRACT: Here, we introduce a 3D-DNA construction method that assembles a minimum number of DNA strands in quantitative yield, to give a scaffold with a large number of single-stranded arms. This DNA frame is used as a core structure to organize other functional materials in 3D as the shell. We use the ring-opening metathesis polymerization (ROMP) to generate block copolymers that are covalently attached to DNA strands. Site-specific hybridization of these DNA-polymer chains on the single-stranded arms of the 3D-DNA scaffold gives efficient access to DNA-block copolymer cages. These biohybrid cages possess polymer chains that are programmably positioned in three dimensions on a DNA core and display increased nuclease resistance as compared to unfunctionalized DNA cages.

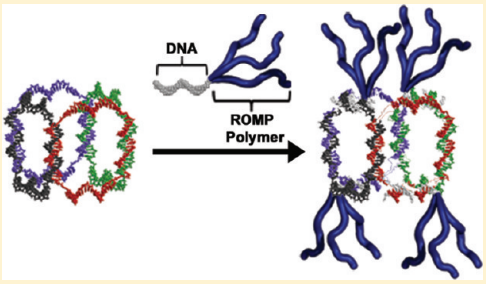

INTRODUCTION

Three-dimensional (3D) DNA structures hold promise for numerous applications, from biological probes and drug delivery tools to organizational scaffolds. Unlike most nanomaterials, they provide fine control over geometry, precise and monodisperse sizes, symmetric or asymmetric positioning of molecules, and molecule-responsive switching of structure.[1−3] Conventional methods to make 3D-DNA structures, such as DNA origami[4−9] or tile-based assembly,[10−17] result in double-stranded, DNA-dense structures.

We were interested in approaching 3D-DNA assembly from an alternative, "DNA-economic" perspective: Can we use a minimum number of DNA strands to create geometrically well-defined 3D-scaffolds, that contain a large number of single-stranded arms? These scaffolds would be able to act as a core structure that guides the site-specific organization of other materials as their shell. This method simply uses DNA to guide other functional structures into three-dimensional arrangements, but the materials generated can be richer in other functionalities than previously reported 3D-DNA structures.

Synthetic polymers are a particularly attractive class of materials with which to "coat" these 3D-DNA scaffolds. They can be engineered for stability, biocompatibility, cell penetrating ability, increased circulation time, and decreased toxicity, and they can introduce multiple functionalities into typically passive DNA structures.[18−21] Polymers with attached DNA strands have previously been made[22,23] and were found to associate into responsive micellar structures and ordered nanofibers.[24−29] Recent work has also explored the use of DNA−polymer conjugates in a number of materials science[30,31] and biological applications.[32−34]

We here report the construction of a new class of biohybrid materials, where synthetic polymer chains are programmably positioned in three-dimensions using DNA cages as scaffolds. A cubic DNA structure, containing eight single-stranded arms, is generated in a facile manner and excellent yield using only a minimum number of component strands. Polymer−DNA conjugates are synthesized through covalent attachment of a ROMP block copolymer to a short DNA strand. These conjugates efficiently hybridize to the individual arms of the DNA scaffolds to produce block-copolymer DNA cages that are more nuclease-resistant than the unfunctionalized DNA cages, making them potential candidates for applications such as responsive biological probes and drug delivery tools.

On a fundamental level, block copolymers are able to undergo self-assembly into a number of useful morphologies, which can be typically controlled by polymer composition, block compatibility, and solvent conditions.[35] The block copolymer-DNA cages shown here introduce new parameters to control morphology, such as the geometry of the DNA scaffold, the 3D-orientation of the polymer chains, and the environmentally responsive nature of DNA assembly. They can thus expand the morphological range that can be obtained from these materials.

RESULTS AND DISCUSSION

Our strategy simplifies the design of 3D-DNA structures and allows for maximized functionality using single-stranded sequences. Figure 1a shows this approach for synthesizing a

Received: November 10, 2011
Published: February 6, 2012

ACS Publications © 2012 American Chemical Society

dx.doi.org/10.1021/ja210313p | J. Am. Chem. Soc. 2012, 134, 4280−4286

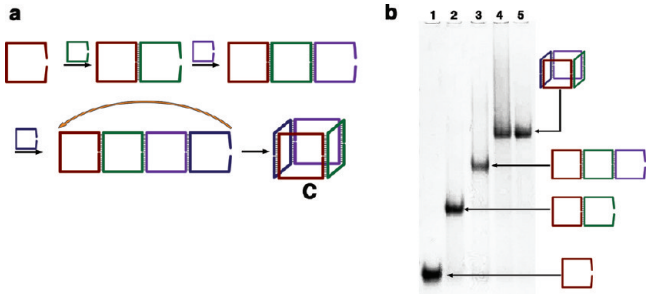

Figure 1. 3D DNA design and assembly. (a) Schematic representation of the stepwise self-assembly of DNA cube **C**. (b) Polyacrylamide gel electrophoresis (PAGE) analysis of **C** assembly under native conditions using four component DNA strands C1−C4: lane 1, C1; lane 2, C1 + C2; lane 3, C1 + C2 + C3; lane 4, C1 + C2 + C3 + C4; and lane 5, C1 + C2 + C3 + C4 after a slow anneal cycle.

DNA cube, illustrating that when one DNA strand hybridizes with the next, its two extremities form a pseudocatenated, cyclic structure. Thus, if a cube is required, four such DNA strands (C1−C4) are connected to each other, with the fourth strand hybridizing to the first to close the cube. Each of these cyclized strands is one face of the final 3D-structure. This approach is inspired by the early and seminal contributions of Seeman and co-workers to 3D DNA assembly.[10] However, in contrast to this initial process, our method results in quantitative assembly yields, does not require ligation steps, and, for the first time, produces 3D-structures with a maximum number of single-stranded regions for further functionalization. Cube **C** is comprised of four 80-nucleotide strands containing four hexanediol (C_6) insertions at the junctions where the structure makes the square faces (see Supporting Information Figure S1 and Table S1 for sequence details and characterization). We previously showed that these insertions increase flexibility and reduce strain, allowing formation of the self-assembled DNA structure in higher yield.

The DNA cube scaffold was synthesized from these component strands at room temperature in a sequential manner and monitored by polyacrylamide gel electrophoresis (PAGE) under native conditions (Figure 1b). Successive additions of the four component strands generated bands of reduced mobility, indicating successful hybridization of each component (lanes 1−4) to produce the 3D nanostructure in excellent yield (lane 4). Heating to 95 °C and slowly cooling the four component strands together in one pot over 3 h yielded quantitative formation of **C** at a final concentration of 1.25 μM (lane 5). Additional experiments also revealed clean assembly of **C** at higher concentrations (5 μM) (see Supporting Information Figure S2). The connectivity of **C** was confirmed using digestion with exonuclease VII (Exo VII). This bidirectional nuclease selectively cleaves single-stranded, open form DNA structures over closed form DNA assemblies. DNA cube **C** did not degrade after Exo VII was added, confirming the closed nature of the assembled 3D-product (see Supporting Information Figure S3).

The assembled DNA cage contains eight single-stranded regions, each 20 bases long, that can be used for further self-assembly (Figure 2a). Each of these regions can possess a different DNA sequence, allowing the independent, site-specific positioning of different functional groups on this frame (see below). In the first iteration of the DNA cube, we simplified the single-stranded regions by introducing sequence symmetry into both the top and the bottom faces. As indicated in Figure 2a,

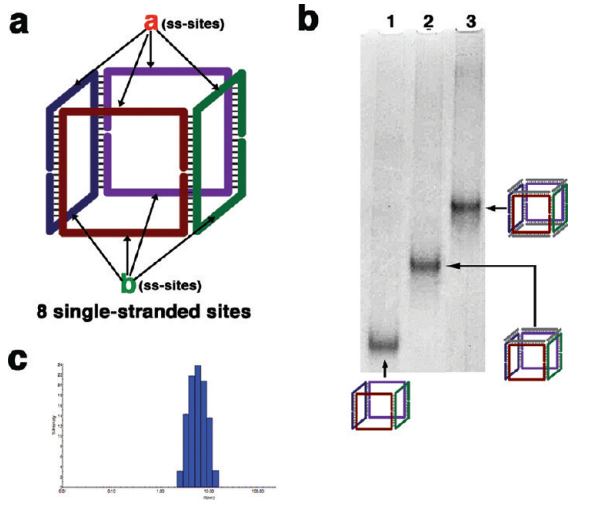

Figure 2. Characterization of DNA cube of **C**. (a) Schematic representation of DNA cube **C** showing sequence symmetry within each single-stranded face. The top face contains 4× sequence **a**, and the bottom face displays 4× sequence **b**. (b) PAGE analysis under native conditions showing the hybridization of complement sequences to the single-stranded DNA regions on the DNA cube: lane 1, **C**; lane 2, **C** + 4×**a**′; lane 3, **C** + 4×**a**′ + 4×**b**′. (c) Dynamic light scattering (DLS) results obtained for single-stranded DNA cube **C**. An average hydrodynamic radius (R_h) of 5.5 ± 0.6 nm was obtained.

each 80 unit strand is designed in such a way that four strands of sequence **a** assemble on one cube face and four strands of sequence **b** assemble on the opposite face. We used PAGE analysis under native conditions to verify that all eight sides are available to hybridize with cDNA strands (Figure 2b). Adding 4 equiv of complementary strand **a**′ to **C** (lane 1) cleanly generates a structure with four occupied sites (lane 2). Adding complementary strand **b**′ yields the fully double-stranded product, called **dsC**, in excellent yield (lane 3). Dynamic light scattering (DLS) was performed to evaluate the physical dimensions of **C** in solution (Figure 1c). An apparent hydrodynamic radius of 5.5 ± 0.6 nm was determined for **C**, which matches well with the calculated theoretical R_h value of 5.8 nm.

The strongest evidence for the formation of the 3D cubic architecture was provided by cryogenic electron microcopy (cryo-EM), a technique that helps to preserve the native environment of self-assembled structures.[5,11,13,17,37] To generate more uniform contrast, we performed cryo-EM imaging on fully double-stranded DNA cube **dsC**, where each of the eight single-stranded regions is hybridized with complementary strands (4× **a**′, 4× **b**′). A typical cryo-EM field of view (Figure 3a) shows numerous single particles, some of which have been enclosed as the areas of contrast within the red squares. Closer inspection of these individual projections reveals a cubic geometry (Figure 3b) that supports the assigned structure, with each area of contrast displaying dimensions that fit one or more of the 20 unit duplex DNA regions of the structures (see Supporting Information Figure S4). In addition, atomic force microscopy (AFM) imaging of **dsC** is consistent across a range of concentrations under dry conditions. A typical AFM field of view (Figure 3c) shows relatively uniform particles with a narrow size distribution. Height measurements on this architecture revealed an average value of 0.6 ± 0.2 nm. The small height value in combination with the ability to see an interior cavity in certain projections indicates that the structure

dx.doi.org/10.1021/ja210313p | J. Am. Chem. Soc. 2012, 134, 4280−4286

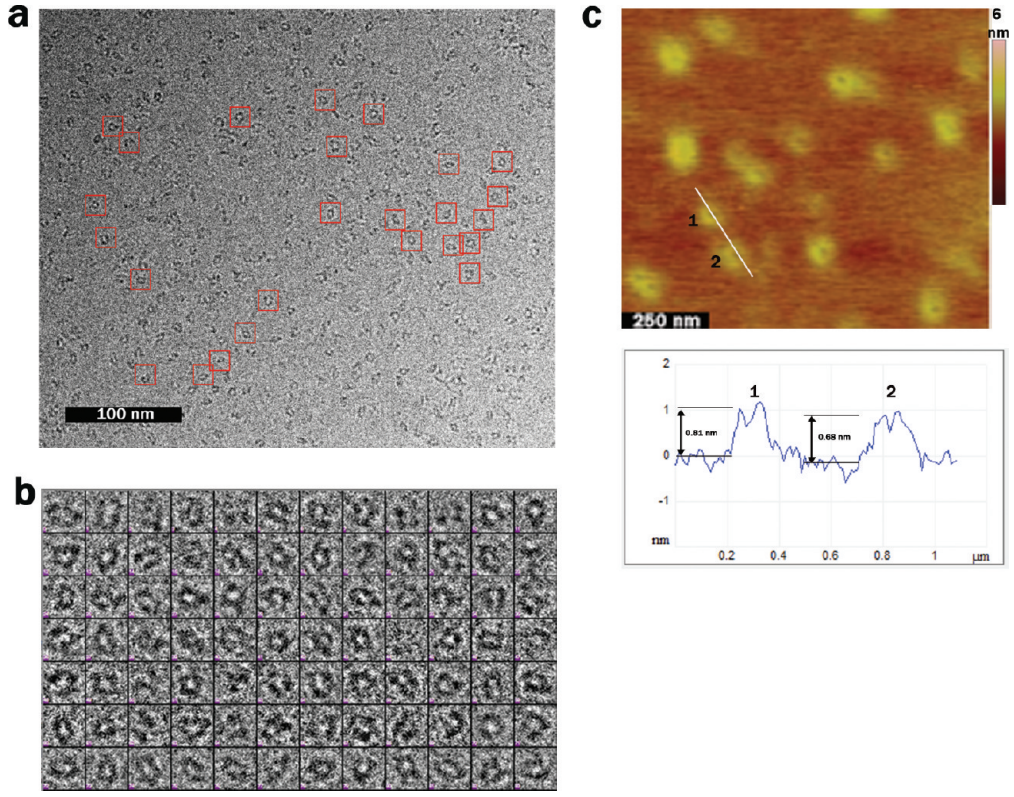

Figure 3. Analysis of DNA cube by cryo-EM and AFM. (a) Typical cryo-EM field of view generated after imaging **dsC** (7 μM). Red boxes enclose areas of contrast that are assigned to the cubic DNA structure. (b) Collected cryo-EM projections that correlate well with the modeled dimensions of **dsC** and reveal detailed facets of the designed cubic structure. (c) Top: Typical AFM field of view (height image) obtained for **dsC** showing the relatively monodisperse nature of the DNA architecture. The white line indicates where a height measurement was taken for structures labeled **1** and **2**. Bottom: Height analysis of structures **1** and **2**.

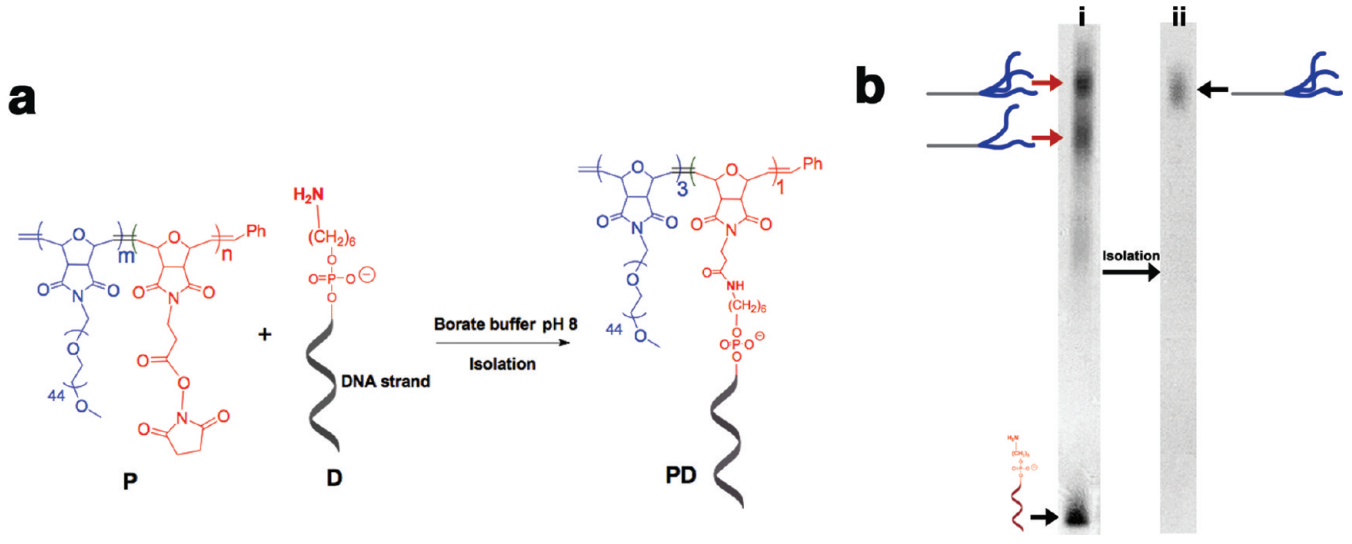

Figure 4. Polymer conjugation to DNA. (a) Schematic representation of the conjugation between amine modified DNA **D** and diblock copolymer **P**. (b) Denaturing PAGE analysis (12%) of the crude conjugation mixture. (i) Black arrow denotes starting material, and red arrows denote major products formed. Isolation of the slowest moving species and reanalysis by PAGE (ii) reveals the pure conjugate product **PD**.

likely strongly adsorbs to the mica substrate and becomes dehydrated to cause flattening.[13,17] Similar results were obtained for single-stranded **C**, although the structures showed less uniform contrast by cryo-EM imaging as compared to **dsC** (Supporting Information Figures S5 and S6).

With the single-stranded DNA cube **C** in hand, we proceeded to construct a DNA block copolymer capable of site-specifically hybridizing to this structure (Figure 4). We first synthesized a short diblock copolymer **P** by living ring-opening metathesis polymerization (ROMP) of ring-strained,[36] substituted oxanorbornene imide monomers (Figure 4a). The first block contains macromonomers, each substituted with a long polyethylene glycol $(PEG)_{44}$ chain, while the second block contains an *N*-hydroxysuccinimide activated carboxylic acid

dx.doi.org/10.1021/ja210313p | *J. Am. Chem. Soc.* 2012, 134, 4280–4286

substituent. Polymerization was carried out using the generation III Grubbs catalyst in dichloromethane under inert atmosphere. NMR analysis revealed a final polymer composition consistent with the monomer to initiator ratio used, and gel permeation chromatography (GPC) showed a narrow molecular weight distribution (polydispersity index PDI = 1.13) (see Supporting Information Figure S7). This data is consistent with the living character of the ROMP reaction used to generate diblock copolymer **P**,[36] now amenable for conjugating to DNA.

Even with a narrow molecular weight distribution, synthetic polymers do not rival the monodisperse nature of biological macromolecules such as DNA. We were therefore interested to find out whether conjugating our ROMP polymers with DNA can help to isolate more monodisperse conjugates. Diblock polymer **P** was reacted with 3′-amine-functionalized DNA strand **D** in a borate buffer (0.1 M, pH 8) at room temperature for 2 days as indicated in Figure 4a. Analysis of the reaction mixture by PAGE under denaturing conditions revealed the presence of two main products significantly retarded in mobility as compared to the amine-DNA starting material (Figure 4b(i), denoted by red arrows). The slowest moving band was isolated to give a clean product, as observed by denaturing PAGE (Figure 4b(ii)). Analysis by matrix assisted laser desorption ionization (MALDI) mass spectrometry indicated a molecular weight that matches the theoretical mass of a $(PEG)_3$–$(DNA)_1$ conjugate, which contains one DNA strand and three PEG repeat units (see Supporting Information Figure S9). Although the yields were moderate for solution-based attachment of DNA to the activated ROMP polymer, the conjugate is more monodisperse due to the uniform nature of DNA, and to the ability to separate the conjugates by gel electrophoresis.

To demonstrate the capacity of our DNA structures for programmable 3D-organization, we designed asymmetric versions of the cube **C1a**–**3a** with precisely positioned binding sites of sequence **a** that are complementary to block copolymer–DNA conjugate **PD** (Figure 5a). Poly(thymidine)

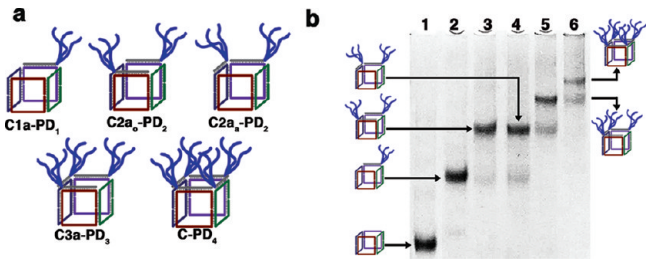

Figure 5. Organizing DNA–polymer conjugate onto 3D DNA scaffold. (a) Schematic representations of DNA cubes with site-specifically arranged polymer conjugate **PD**. (b) Native PAGE analysis of cubes **C1a**–**3a** hybridized to DNA–polymer conjugate **PD**: lane 1, **C**; lane 2, **C1a** + 1 equiv of **PD**; lane 3, $\mathbf{C2a_o}$ + 2 equiv of **PD**; lane 4, $\mathbf{C2a_a}$ + 2 equiv of **PD**; lane 5, **C3a** + 3 equiv of **PD**; and lane 6, **C** + 4 equiv of **PD**.

tracts (T_{14}, denoted as **X**) were incorporated into specific single-stranded positions of the cubes to eliminate binding of polymer–DNA conjugate **PD**. Structure **C1a**, containing only one binding site, was first hybridized with 1 equiv of the **PD**. This resulted in a single band by PAGE under native conditions (Figure 5b, lane 2) with reduced mobility as compared to unsubstituted cube **C** (Figure 5b, lane 1). This structure was assigned to the singly substituted cube $\mathbf{C1a\text{-}PD_1}$, with one site occupied by PEG_3-ROMP polymer **P**. We also confirmed the availability of PD for hybridization through stoichiometric association with the complement strand (Supporting Information Figure S9).

Because of the programmability of the single-stranded regions, two **a** binding sites could be positioned in either an opposite ($\mathbf{C2a_o}$) or an adjacent ($\mathbf{C2a_a}$) orientation within a cubic face. Hybridization with 2 equiv of **PD** to $\mathbf{C2a_o}$ (Figure 5b, lane 3) gave a near quantitative yield of a single band of reduced mobility as compared to the monosubstituted cube, indicating that a DNA cube had been generated with two PEG_3- ROMP polymers site-specifically positioned on opposite faces ($\mathbf{C2a_o\text{-}PD_2}$). Adding the DNA–polymer conjugate to $\mathbf{C2a_a}$ also generated disubstituted cube $\mathbf{C2a_a\text{-}PD_2}$ in good yield (Figure 5b, lane 4). A small amount of monosubstituted cube was observed in this case, suggesting that the six adjacent PEG chains on this cube may be sterically crowded, thus slightly reducing the yield.

When a cube containing three adjacent binding sites (**C3a**) was hybridized with 3 equiv of **PD**, a major band that is assigned to trisubstituted cube $\mathbf{C3a\text{-}PD_3}$ with nine PEG_{44} chains was observed, along with a minor band with the same mobility as a disubstituted cube (Figure 5b, lane 5). With four adjacent binding sites (**C**), tetrasubstituted cube $\mathbf{C\text{-}PD_4}$ with 12 PEG_{44} chains was obtained, showing a more sizable band for a trisubstituted byproduct (Figure 5b, lane 6). As a control, 20 equiv of **PD** was added to **C** and resulted in no change to the product distribution, indicating that stoichiometry was not a contributing factor (see Supporting Information Figure S10). The trend in electrophoretic mobilities for each polymer-bound 3D-DNA architecture indicates that sterics may influence hybridization, especially when binding sites are arranged in an adjacent fashion.

To test how orientation of the single-stranded regions may influence hybridization to our DNA–polymer conjugate, we designed a cubic structure $\mathbf{C4a_o}$ that orients sequence **a** on opposite sides of the top and bottom cubic faces as depicted in Figure 6a. Such an arrangement could help to offset the steric effects from DNA–polymer conjugate binding. As compared to binding two polymer–DNA conjugates (Figure 6b, lane 1), native PAGE analysis of this new arrangement reveals a major band that can be assigned to cube $\mathbf{C4a_o\text{-}PD_4}$ with four polymers bound (lane 2), and a smaller amount of the triply bound species.

In addition to PAGE, DLS studies show that DNA cube size increases as varying amounts of polymer are added (see Supporting Information Figures S11 and S12 and Table S3). The average experimental R_h values of 8.9 ± 1.0 nm ($\mathbf{C2a_o\text{-}PD_2}$) and 10.5 ± 1.2 nm ($\mathbf{C4a_o\text{-}PD_4}$). These results indicate successful hybridization of the DNA–polymer conjugate onto the 3D-DNA scaffold. AFM imaging of the site-specifically organized DNA–polymer conjugates onto **C** also displayed distinct differences depending on the architecture being imaged. Samples of $\mathbf{C2a_o\text{-}PD_2}$ and $\mathbf{C4a_o\text{-}PD_4}$ were prepared at both 10 and 50 nM concentrations for AFM imaging (see Supporting Information Figures S13–S16). At 50 nM, aggregates were observed, likely the result of interactions between the polymer chains organized onto the DNA scaffolds and drying effects on the mica surface. Analysis of these particles revealed average heights of 1.5 ± 0.3 nm ($\mathbf{C2a_o\text{-}PD_2}$) and 2.2 ± 0.4 nm ($\mathbf{C4a_o\text{-}PD_4}$). In an effort to reduce aggregation effects, $\mathbf{C4a_o\text{-}PD_4}$ and $\mathbf{C4a_o\text{-}PD_4}$ were imaged at 10 nM (Figure 6c and d). Fewer aggregate domains were

dx.doi.org/10.1021/ja210313p | J. Am. Chem. Soc. 2012, 134, 4280–4286

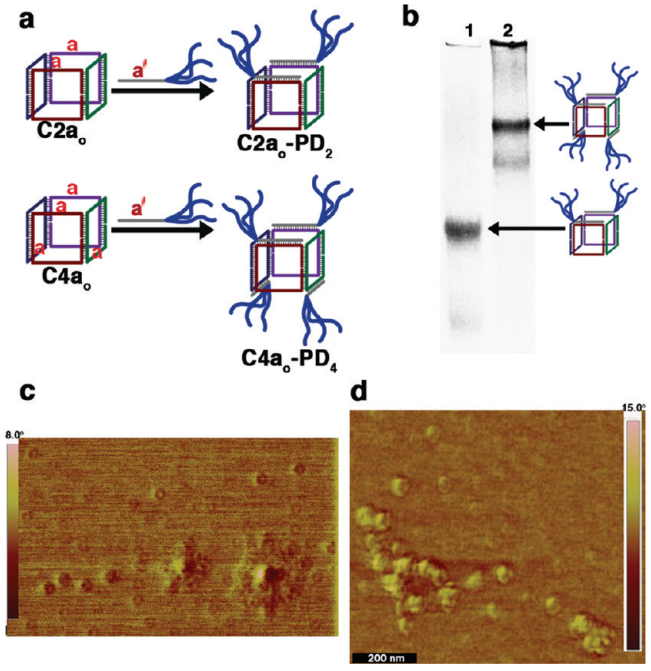

Figure 6. Programmable organization of DNA–polymer conjugates onto a 3D scaffold. (a) To help reduce sterics and maximize the number of DNA–polymer conjugates bound to the DNA cube, structure **C4a$_o$** was designed to place two single-stranded sites on one cubic face and two sites perpendicular to these on the opposite face. (b) Native PAGE analysis of DNA-containing cubes **C2a$_o$-PD$_2$** (lane 1, 2 equiv of **PD**) and **C4a$_o$-PD$_4$** (lane 2, 4 equiv of **PD**). (c) AFM image obtained for **C2a$_o$-PD$_2$** (10 nM). Phase image shown. (d) AFM image obtained for **C4a$_o$-PD$_4$** (10 nM). Phase image shown.

observed, and analysis at this concentration produced height values of 0.8 ± 0.1 nm (**C2a$_o$-PD$_2$**) and 0.9 ± 0.20 nm (**C4a$_o$-PD$_4$**). Taking into consideration an average height of 0.6 ± 0.2 nm recorded for DNA-only structure **dsC**, overall height comparisons between **C2a$_o$-PD$_2$** and **C4a$_o$-PD$_4$** support the site-specific organization of the DNA–polymer conjugate **PD** onto these 3D DNA scaffolds. To our knowledge, these studies constitute the first examples of using three-dimensional scaffolds to organize block copolymers in a programmable way in 3D-space. This approach is expected to significantly increase the morphological range possible with block copolymers.

To gain insight into the sensitivity of our DNA cube to nucleases, with and without organized synthetic polymer, we studied these architectures under conditions that mimic the physiological environment. Each structure (**C**, **C2a$_o$-PD$_2$**, and **C4a$_o$-PD$_4$**) was prepared and subjected to digestion with a 10% solution (v/v) of fetal bovine serum (FBS), which contains a milieu of nonspecific nucleases commonly found in the in vitro assays. A control double-stranded DNA **NC** was digested by FBS (37 °C) in 2 h (see Supporting Information Figure S17). The single-stranded DNA structure **C** shows a similar FBS digestion profile (see Supporting Information Figure S17) as compared to **NC**. We next looked at the nuclease profile of structures where the synthetic polymer had been site-specifically organized onto the 3D-DNA scaffold. Analysis of **C2a$_o$-PD$_2$** after addition of 10% FBS revealed a digestion pattern (Figure 7a) similar to that of **C**. The 80-nucleotide component strands were digested by the 4 h time point, indicating that functionalization with two polymers is not

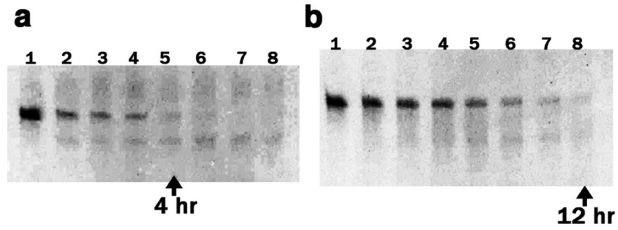

Figure 7. FBS digestion of **C2a$_o$-PD$_2$** and **C4a$_o$-PD$_4$**. Denaturing PAGE analysis (12%) of time points taken from FBS assay preformed on (a) **C2a$_o$-PD$_2$** and (b) **C4a$_o$-PD$_4$**. In each experiment: lane 1, 0 h; lane 2, 0.5 h; lane 3, 1 h; lane 4, 2 h; lane 5, 4 h; lane 6, 6 h; lane 7, 8 h; and lane 8, 12 h.

sufficient to prevent nuclease activity. On the other hand, structure **C4a$_o$-PD$_4$**, which displays two polymers on each single stranded face, shows more stability up to a 12 h time point, as evidenced by the continued presence of the component strands (Figure 7b). We are currently exploring further nuclease analysis and developing methods to block or functionalize the nicked sections of the cube structure, thus increasing long-term stability. These nuclease results are encouraging, in that the specific arrangement of polymers on two of the cubic faces is sufficient to hinder nuclease binding. Ultimately, this feature will help to extend the lifetime of such structures in drug delivery and bioimaging applications.[38–40]

■ CONCLUSIONS

We have introduced a method to build 3D-DNA structures that represents a departure from previous approaches. It starts with a minimum number of DNA strands, and assembles these in quantitative yield, to give a 3D-scaffold that contains a large number of single-stranded arms. This well-defined 3D-DNA "frame" can then be used as a core structure onto which a number of other materials can be patterned, to create core–shell biohybrid structures. We used the ring-opening metathesis polymerization (ROMP) to generate block copolymers that are covalently attached to a DNA strand. Site-specific hybridization of these DNA-polymer chains on the single-stranded arms of the 3D-DNA scaffold gives efficient access to a range of biohybrid DNA-block copolymer cages, where single polymer chains are programmably positioned in three dimensions on a DNA core. We find that these polymer-coated DNA cages are more nuclease-resistant than the unfunctionalized DNA structures. Thus, these DNA-programmed block copolymers structures bring together the functionality, biocompatibility, and self-assembling potential of block copolymers with the fine control of geometry, positioning, and responsive character of DNA cages. As such, they will be a promising platform for exploring new applications in biology and materials science.

■ EXPERIMENTAL SECTION

Assembly of DNA Cube C. Equimolar amounts of strands **C1–C4** (250 pmol each) were dried down together and then redissolved in 200 μL of 1xTAEMg buffer. This mixture was then subjected to an annealing protocol whereby strands were held at 95 °C for 5 min, then 80 °C for 3 min, cooled to 60 °C (2 min/°C), and finally slowly cooled to 4 °C (3 min/°C). Final cube concentration was ca. 1.25 μM. Cubes **C1a–3a** and **C4a$_o$** were prepared in an identical manner (see Supporting Information Tables S1 and S2).

Polymer Synthesis. Unless otherwise stated, all reagents and solvents were purchased from Sigma-Aldrich Chemicals and used without further purification, and all reactions were carried out under an atmosphere of nitrogen at room temperature. Monomers **S1** and **S2**

dx.doi.org/10.1021/ja210313p | J. Am. Chem. Soc. 2012, 134, 4280–4286

were prepared according to literature procedures. A dry Schlenk tube was charged with Grubbs' catalyst third generation (100.0 mg, 0.112 mmol, 1 equiv) under an argon atmosphere. Dry CH_2Cl_2 (5 mL) was added, and the mixture was stirred at room temperature for 5 min (Figure S5). A solution of NHS-monomer (**S1**, 39.3 mg, 0.112 mmol, 1 equiv) in dry CH_2Cl_2 (5 mL) was added, and the mixture was stirred for 30 min. A solution of PEG-monomer (**S2**, 731.9 mg, 0.338 mmol, 3 equiv) in dry CH_2Cl_2 (5 mL) was then added, and the reaction mixture was stirred for another 30 min before ethyl vinyl ether (1 mL, excess) was added to quench the polymerization (Scheme 1). The polymer was precipitated with petroleum ether (716 mg, 94%) and purified by column chromatography (CH_2Cl_2–MeOH 100:0 to 80:20): polymer **P** (234 mg, 31%) was obtained as a brown amorphous solid. Ruthenium-containing byproduct was removed by successive extraction of an aqueous solution of polymer (10 mL) with $CHCl_3$–isopropyl alcohol 3:1 (3 × 10 mL). Organic layers were combined, dried ($MgSO_4$), filtered, and concentrated under reduced pressure to afford the pure polymer **P** as a light brown solid. ^{1}H NMR (400 MHz, CD_2Cl_2, 298 K): δ = 7.44 (d, J = 6.1 Hz, 2H, H_B), 7.34 (t, J = 7.1 Hz, 2H, H_C), 7.28 (q, J = 6.8 Hz, 1H, H_A), 6.75 (d, J = 15.7 Hz, 1H, H_D), 6.35 (dd, J = 3.3, 15.7 Hz, 1H, H_E), 5.95–6.15 (m, 6H, H_F and H_G), 5.80 (bd, J = 5.5 Hz, 1H, H_I), 5.44 (d, J = 17.0 Hz, 1H, $H_{I'}$), 4.87–5.06 (m, 2H, $H_{\alpha'}$ and $H_{\beta'}$), 4.33–4.62 (m, 6H, H_α and H_β), 3.77 (t, J = 4.3 Hz, 6H, $H_{a'}$), 3.45–3.45 (m, 530H, H_a, $H_{c'}$, and $H_{d'}$), 3.33 (s, 9H, $H_{e'}$), 2.80 (s, 4H, H_c), 2.67 (bt, J = 6.0 Hz, 2H, H_b), 1.93–2.10 (m, 2H, $H_{\gamma'}$ and $H_{\delta'}$), 1.65–1.84 (m, 6H, H_γ and H_δ). GPC (DMF, 1 mL/min): Mp = 6678, PDI = 1.13. See Supporting Information Figure S5 for GPC trace and ^{1}H NMR spectrum.

Scheme 1

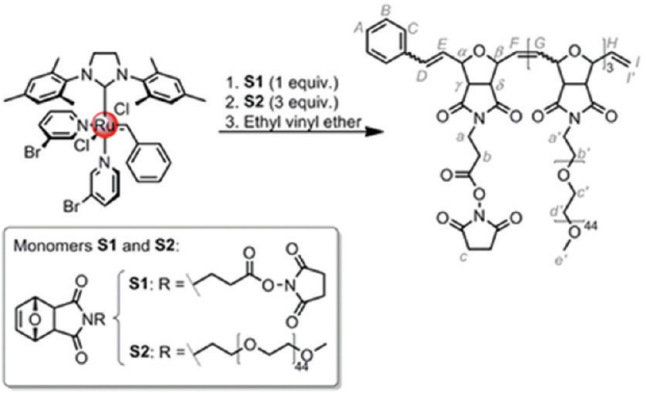

DNA–Polymer Conjugation. In a typical conjugation reaction, 200 nmol of 3′-amine DNA (sequence **D**) was dried down under reduced pressure and heat. The DNA was then resuspended in 50 μL of a borate buffer (0.1 M, pH 8). NHS-activated polymer **P** (1 μmole) was weighed out in a 0.5 mL microcentrifuge tube and completely dissolved in 50 μL of acetonitrile. The DNA solution was then transferred to this tube, mixed, and allowed to react at room temperature for 2 days with agitation. The reaction mixture was reduced to dryness and dissolved in 75 μL of H_2O. Urea (8 M, 75 μL) was then added, and the mixture was loaded onto a 12% denaturing PAGE gel. The major product was purified by the crush and soak method, desalted using size exclusion chromatography (Sephadex G-25), and quantified (OD_{260}) using UV–vis spectroscopy.

Annealing DNA–Polymer Conjugate PD to 3D DNA Cubes. In a typical assembly (Figure S8a), DNA cube **C** (4 μL, 1.25 μM) was pipetted into a 0.5 mL microcentrifuge tube. DNA–polymer conjugate **PD** (1 μL, 20 μM) was added to **C** with slight mixing. 1xTAEMg buffer (5 μL) was added to make the final cube concentration 0.5 μM, and the mixture was allowed to stand at room temperature for 10 min. For each of the cubes containing poly(thymidine) tracts, the amount of DNA–polymer conjugate and 1xTAEMg buffer added was modified according to the number of binding sites available.

■ ASSOCIATED CONTENT

Ⓢ Supporting Information

Chemicals and materials, detailed experimental procedures, 3D component sequences, characterization methods, and supplemental figures. This material is available free of charge via the Internet at http://pubs.acs.org.

■ AUTHOR INFORMATION

Corresponding Author

hanadi.sleiman@mcgill.ca

Notes

The authors declare no competing financial interest.

■ ACKNOWLEDGMENTS

We thank NSERC, CFI, CSACS, CIFAR and the SNF for financial support, and Dr. Isabelle Rouiller and Dr. Minhea Bostina for assistance with cryo-EM imaging. Parts of this manuscript, specifically polymer synthesis and conjugation, were made possible by NPRP from the Qatar National Research Fund (a member of Qatar Foundation). The statements made herein are solely the responsibility of the authors. H.F.S. is a Cottrell Scholar of the Research Corporation.

■ REFERENCES

(1) Seeman, N. C. *Nature* **2009**, *421*, 427.
(2) Aldaye, F. A.; Palmer, A. L.; Sleiman, H. F. *Science* **2009**, *321*, 1795.
(3) Lin, C.; Liu, Y.; Yan, H. *Biochemistry* **2009**, *48*, 1663.
(4) Rothemund, P. W. *Nature* **2006**, *440*, 297.
(5) Andersen, E. S.; et al. *Nature* **2009**, *459*, 73.
(6) Douglas, S. M.; Dietz, H.; Liedl, T.; Högberg, B.; Graf, F.; Shih, W. M. *Nature* **2009**, *459*, 414.
(7) Ke, Y.; Sharma, J.; Liu, M.; Jahn, K.; Liu, Y.; Yan, H. *Nano Lett.* **2009**, *9*, 2445.
(8) Endo, M.; Hidaka, K.; Kato, T.; Namba, K.; Sugiyama, H. *J. Am. Chem. Soc.* **2009**, *131*, 15570.
(9) Han, D.; Pal, S.; Nangreave, J.; Deng, Z.; Liu, Y.; Yan, H. *Science* **2011**, *332*, 342.
(10) Chen, J. H.; Seeman, N. C. *Nature* **1991**, *350*, 631.
(11) Shih, W. M.; Quispe, J. D.; Joyce, G. F. *Nature* **2004**, *427*, 618.
(12) Goodman, R. P.; Schaap, I. A.; Tardin, C. F.; Erben, C. M.; Berry, R. M.; Schmidt, C. F.; Turberfield, A. J. *Science* **2005**, *310*, 1661.
(13) He, Y.; Ye, T.; Su, M.; Zhang, C.; Ribbe, A. E.; Jiang, W.; Mao, C. *Nature* **2008**, *452*, 198.
(14) Andersen, F. F.; et al. *Nucleic Acids Res.* **2008**, *36*, 1113.
(15) Zimmermann, J.; Cebulla, M. P.; Monninghoff, S.; von Kiedrowski, G. *Angew. Chem., Int. Ed.* **2008**, *47*, 3626.
(16) Bhatia, D.; Mehtab, S.; Krishnan, R.; Indi, S. S.; Basu, A.; Krishnan, Y. *Angew. Chem., Int. Ed.* **2009**, *48*, 4134.
(17) Severcan, I.; Geary, C.; Chworos, A.; Voss, N.; Jacovetty, E.; Jaeger, L. *Nat. Chem.* **2010**, *2*, 772.
(18) Fuks, G.; Talom, R. M.; Gaufree, F. *Chem. Soc. Rev.* **2011**, *40*, 2475.
(19) Vicent, M. J.; Dieudonne, L.; Carbajo, R. J.; Pineda-Lucena, A. *Expert Opin. Drug Delivery* **2008**, *5*, 593.
(20) van Dongen, S. F. M.; de Hoog, H.-P.M.; Peters, R. J. R. W.; Nallani, M.; Nolte, R. J. M.; van Hest, J. C. M. *Chem. Rev.* **2009**, *109*, 6212.
(21) Hawker, C. J.; Wooley, K. L. *Science* **2005**, *309*, 1200.
(22) Watson, K. J.; Park, S.; Im, J.; Nguyen, S. T.; Mirkin, C. A. *J. Am. Chem. Soc.* **2001**, *123*, 5592.
(23) Kwak, M.; Herrmann, A. *Angew. Chem., Int. Ed.* **2010**, *49*, 8574.
(24) Li, Z.; Zhang, Y.; Fullhart, P.; Mirkin, C. A. *Nano Lett.* **2004**, *4*, 1055.

(25) Gibbs-Davis, J. M.; Schatz, G. C.; Nguyen, S. T. *J. Am. Chem. Soc.* **2007**, *129*, 15535.
(26) Ding, K.; Alemdaroglu, F. E.; Borsch, M.; Berger, R.; Herrmann, A. *Angew. Chem., Int. Ed.* **2007**, *46*, 1172.
(27) Chien, M.; Rush, A. M.; Thompson, M. P.; Gianneschi, N. C. *Angew. Chem., Int. Ed.* **2010**, *49*, 5076.
(28) Kwak, M.; Minten, I. J.; Anaya, D.-M.; Musser, A. J.; Brasch, M.; Nolte, R. J. M.; Müllen, K.; Cornelissen, J. J. L. M.; Herrmann, A. *J. Am. Chem. Soc.* **2010**, *132*, 7834.
(29) Pan, P.; Fujita, M.; Ooi, W.-Y.; Sudesh, K.; Takarada, T.; Goto, A.; Maeda, M. *Polymer* **2011**, *52*, 895.
(30) Chien, M.-P.; Gianneschi, N. C. *Small* **2011**, *7*, 2041.
(31) Kwak, M.; et al. *Angew. Chem., Int. Ed.* **2010**, *50*, 3206.
(32) Jeong, J. H.; Park, T. G. *Bioconjugate Chem.* **2001**, *12*, 917.
(33) Alemdaroglu, F. E.; Alemdaroglu, N. C.; Langguth, P.; Herrmann, A. *Adv. Mater.* **2008**, *20*, 899.
(34) Patwa, A.; Gissot, A.; Bestel, I.; Barthelemy, P. *Chem. Soc. Rev.* **2011**, DOI: 10.1039/c1cs15038c.
(35) Giacomelli, C.; Schmidt, V.; Aissou, K.; Borsali, R. *Langmuir* **2010**, *26*, 15734.
(36) Sankaran, N. B.; Rys, A. Z.; Nassif, R.; Nayak, M. K.; Metera, K.; Chen, B.; Bazzi, H. S.; Sleiman, H. F. *Macromolecules* **2010**, *43*, 5530.
(37) Kato, T.; Goodman, R. P.; Erben, C. M.; Turberfield, A. J.; Namba, K. *Nano Lett.* **2009**, *9*, 2747.
(38) Ko, S.; Liu, H.; Chen, Y.; Mao, C. *Biomacromolecules* **2008**, *9*, 3039.
(39) Bhatia, D.; Surana, S.; Chakraborty, S.; Koushika, S. P.; Krishnan, Y. *Nat. Commun.* **2011**, *2*, 339.
(40) Walsh, A. S.; Yin, H.; Erben, C. M.; Wood, M. J. A.; Turberfield, A. J. *ACS Nano* **2011**, *5*, 5427.